

Mechanical properties of tracheal tubes in the American cockroach (*Periplaneta americana*)

Matthew R Webster^{1,4}, Raffaella De Vita¹, Jeffrey N Twigg²
and John J Socha³

¹ Mechanics of Soft Biological Systems Laboratory, Department of Engineering Science and Mechanics, Virginia Tech, Blacksburg, VA 24061, USA

² Army Research Laboratory, 2800 Powder Mill Road, Adelphi, MD 20783, USA

³ Department of Engineering Science and Mechanics, Virginia Tech, Blacksburg, VA 24061, USA

E-mail: mwbstr@vt.edu, devita@vt.edu, jeffrey.n.twigg@us.army.mil and jjsocha@vt.edu

Received 28 January 2011, in final form 6 May 2011

Published 30 August 2011

Online at stacks.iop.org/SMS/20/094017

Abstract

Insects breathe using an extensive network of flexible air-filled tubes. In some species, the rapid collapse and reinflation of these tubes is used to drive convective airflow, a system that may have bio-inspired engineering applications. The mechanical behavior of these tracheal tubes is critical to understanding how they function in this deformation process. Here, we performed quasi-static tensile tests on ring sections of the main thoracic tracheal trunks from the American cockroach (*Periplaneta americana*) to determine the tracheal mechanical properties in the radial direction. The experimental findings indicate that the stress–strain relationships of these tracheal tubes exhibit some nonlinearities. The elastic modulus of the linear region of the stress–strain curves tubes was found to be 1660 ± 512 MPa. The ultimate tensile strength, ultimate strain and toughness were found to be 23.7 ± 7.33 MPa, $2.0 \pm 0.7\%$ and 0.207 ± 0.153 MJ m⁻³, respectively. This study is the first experimental quantification of insect tracheal tissue, and represents a necessary step toward understanding the mechanical role of tracheal tubes in insect respiration.

(Some figures in this article are in colour only in the electronic version)

1. Introduction

Insects are capable of physiological feats unmatched by engineered systems. In flight, insects such as dragonflies are capable of flying forward, backward, upward, downward, and side-to-side [20]. The principles governing their performance have fascinated engineers and inspired the development of novel micro air vehicles [4, 23], but insects remain far superior in maneuverability, control, and power consumption. The range of behaviors worthy of engineering inspiration from insects is also apparent in the unique defensive mechanisms of some species [6]. For example, the bombardier beetles are able to fire a noxious, boiling hot mix of chemicals to blast

their predators. The process by which these beetles produce and expel these chemicals has inspired the design of new spray technologies used in car engines, fire extinguishers, and drug delivery devices [12]. The intelligent control systems of cockroaches in locomotion on rough terrain have been long appreciated and applied to hexapod robots [2, 1]. Despite such research and application, many aspects of insect biology remain unexplored as a source of inspiration.

One such physiological system that has received little attention from engineers is the insect respiratory system. Insects are capable of massive modulations of metabolic rate [3], which can be more than an order of magnitude higher than those seen in vertebrate animals. An important component of this performance is the design of the tracheal system, which supports both diffusion- and convective-based gas transport. This respiratory system consists of a network of air-filled

⁴ The authors are listed in the order of importance of their individual contributions to the work.

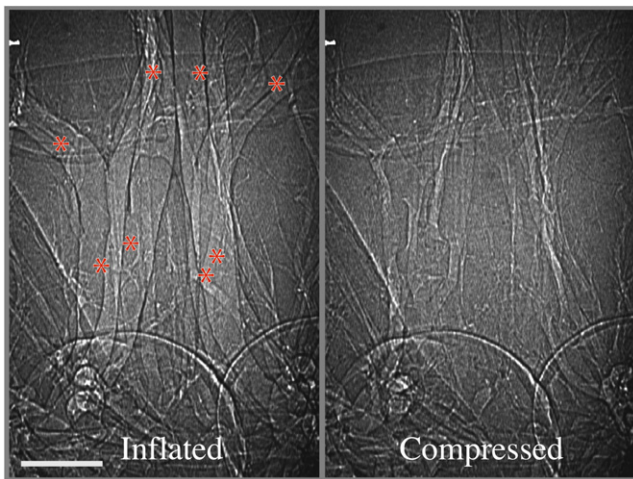


Figure 1. Representative example of tube collapse in rhythmic tracheal compression in the prothoracic tracheal tubes of the beetle *Pterostichus stygicus*, from [16]. Scale bar, 200 μm .

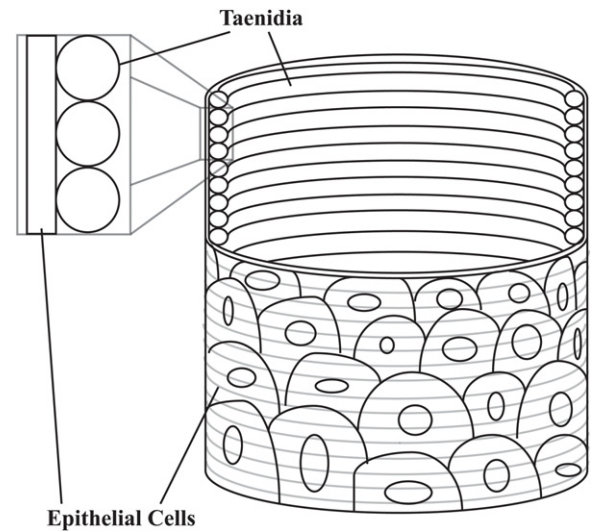


Figure 2. Generalized schematic of insect tracheal tubes, showing circumferentially oriented taenidia.

tubes and sacs that permeate the entire body. The internal tracheal tubes are connected to the external environment through valve-like structures, known as spiracles, located along the exoskeleton. Oxygen-rich air is delivered directly to the cells, without requiring blood circulation, through thin-walled micron-scale tracheal tubes known as tracheoles [8]. Early investigations on the insect respiratory system suggested that for some insects gas exchange could be achieved solely by diffusion [9, 21], but many insects supplement diffusion with convective transport [13].

One mechanism for producing convective flows of air in the respiratory system is by deforming the tracheal structures to reduce volume, thereby pumping air via volume displacement. The dynamics of such deformation in living insects have been studied in recent years using synchrotron x-ray imaging methods [17, 16, 22]. One behavior of interest is termed ‘rhythmic tracheal compression’ (RTC), in which parts of the tracheal system synchronously collapse and reinflate on the order of 10–20 times min^{-1} [17, 22]. Only parts of the tracheal system collapse—not every tube participates, and in tubes that do collapse, some locations remain inflated, with the net effect being a complex pock-mark-like pattern (figure 1). Although little is known about the mechanism of compression or its exact physiological role in insect gas exchange [15], it is abundantly clear that there is currently no engineering analog to this system. In insects that use RTC, airflows are produced with hundreds of simultaneous compressions of a complex, soft tissue network. The mechanical principles that underly this flow generation may lead to advances in microfluidics or tissue engineering, where issues of efficient nutrient delivery are tantamount to successful design. However, the development of any device inspired by insect respiratory systems requires a thorough understanding of their mechanics.

The rhythmic and selective collapse behavior of tracheal tubes in RTC is made possible by the inherent structure of these tubes. Insect tracheal tubes are composed of two distinct layers: an outer layer of epithelial cells and an inner layer of chitin fibers embedded in a matrix known as the intima

layer [11, 8] (figure 2). The epithelial cells in the outer layer secrete mainly chitin and other proteins but likely do not play any mechanical role. In the region adjacent to the outer layer, there is a layer of chitin fibers aligned longitudinally. The inner layer consists of spirally or circumferentially wound thickenings of chitin fibers, known as taenidia, which provide structural support to the tracheal tubes. In particular, the taenidia give compressive resistance to the tracheal tubes, but their spiral or circumferential configuration likely enables them to deform and be restored to their pre-compression, fully inflated shape.

The chitin fibers, which are the main structural component of the insect tracheal tubes, are also abundant in the cuticle of the exoskeleton [19], providing structural support, mobility, and protection to the body. The cuticle acts as a rigid framework in some areas such as the tibia and the mandibles, and yet provides mobility at the joints due to a variation in its mechanical properties known as functional grading, in which the material properties change continuously along the body. The cause of the variation in the mechanical properties is a combination of different factors: the volume fraction and alignment of chitin, the composition of the surrounding matrix material, and the level of hydration [18]. Functional grading in insect tracheal tubes may also be responsible for their selective collapse during respiration.

Experimental studies are necessary to characterize the mechanical behavior of insect tracheal tubes, both to understand their role in respiration and to provide a basis for future bio-inspired engineering designs that borrow principles from insect tracheal networks. However, to our knowledge, there have been no studies of the mechanical properties of insect tracheal tubes. Basic material properties such as elastic modulus, ultimate tensile strength, ultimate strain and toughness of insect tracheae have yet to be determined. In this study, we quantified the mechanical properties of the main anterior thoracic tracheal trunks of the American cockroach (*Periplaneta americana*). Specifically, we isolated

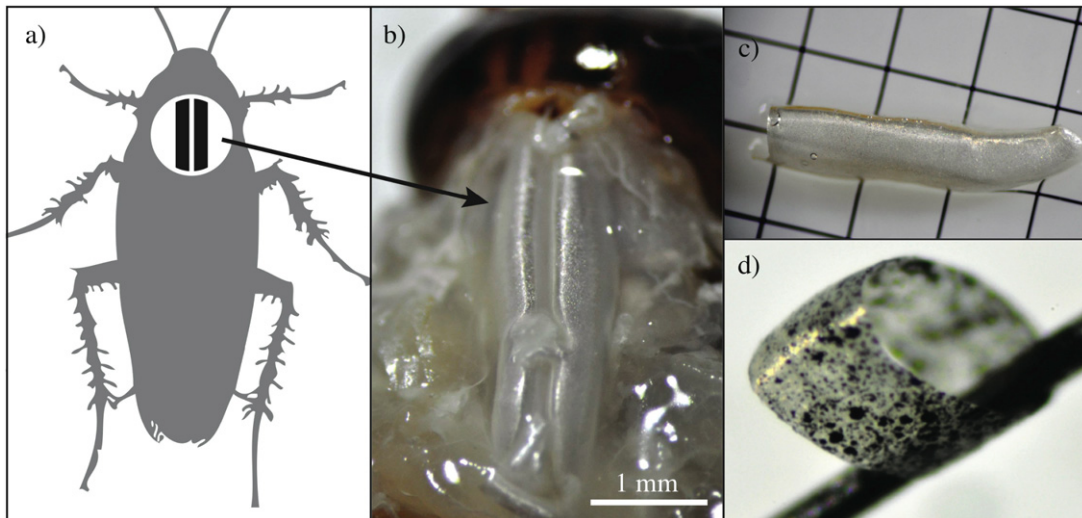


Figure 3. (a) Location of main thoracic tracheal trunks in the American cockroach. (b) Main thoracic tracheal trunks. (c) Dissected tracheal tube. (d) Speckle coated section of tracheal tube.

ring sections from these tubes and conducted tensile testing in the radial direction. Understanding the properties of these soft, flexible tubes represents a necessary first step toward any bio-inspired engineering application of rhythmic tracheal compression and other mechanisms of insect respiration.

2. Experimental methods

2.1. Specimen preparation

Tracheal tubes from eleven male American cockroaches (*Periplaneta americana*; mass = 0.823 ± 0.15 g, length = 32.9 ± 1.83 mm; mean \pm SD) were used in this study. Cockroaches were acquired from the Virginia Tech Department of Entomology and housed in a colony with *ad libitum* food and water prior to testing. The four large primary tracheal trunks, located just posterior to the head in the upper thorax, were tested. These particular tracheal tubes were chosen for their large size and relative uniformity of diameter.

To extract the tracheal tubes, the cockroaches were first sacrificed with fumes of ethyl acetate. Within an hour, the dorsal thoracic exoskeleton was removed, revealing the four main tracheal trunks in the thorax (figures 3(a) and (b)). The tracheal tubes were extracted under a dissection stereoscope (Zeiss Stemi 2000-C Stereoscope) and were placed immediately in a bath containing physiological insect Ringer's solution (0.75 g NaCl, 0.35 g KCl, 0.28 g CaCl₂, 1 l distilled water) [10] to maintain hydration. Ring sections of roughly equal length were cut manually using a scalpel. As much as possible, sections were chosen with nearly constant diameter along the width and taenidia aligned consistently in the radial direction.

Prior to testing, the width, thickness (as defined in figure 4(a)) and diameter of the ring sections were measured optically using images taken by a digital camera (Nikon D-5000). The measurement error was determined to be $\pm 0.2 \mu\text{m}$ based on the camera resolution (4288×2848) and the level of magnification of the stereoscope ($30\times$). From the thirty

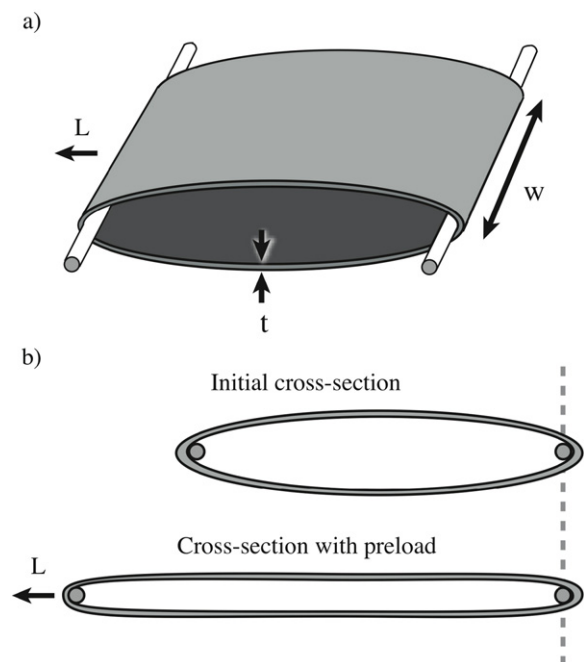


Figure 4. (a) Schematic of a ring test. (b) Effect of pre-loading during testing. The cylindrical surface of the specimen becomes more planar under load.

ring sections selected for stress and strain analyses, the width, thickness and diameter were found to be $360 \pm 70 \mu\text{m}$, $7.1 \pm 0.4 \mu\text{m}$ and $800 \pm 120 \mu\text{m}$, respectively. The surface of the ring specimens was speckle coated with black ink using an airbrush (Badger Model 150), which was applied to produce suitable contrast for strain measurements. The specimens were kept in Ringer's solution until testing.

2.2. Testing apparatus and protocol

A new testing system (figure 5(a)) was designed and built to measure the tensile properties of tracheal tubes in the radial

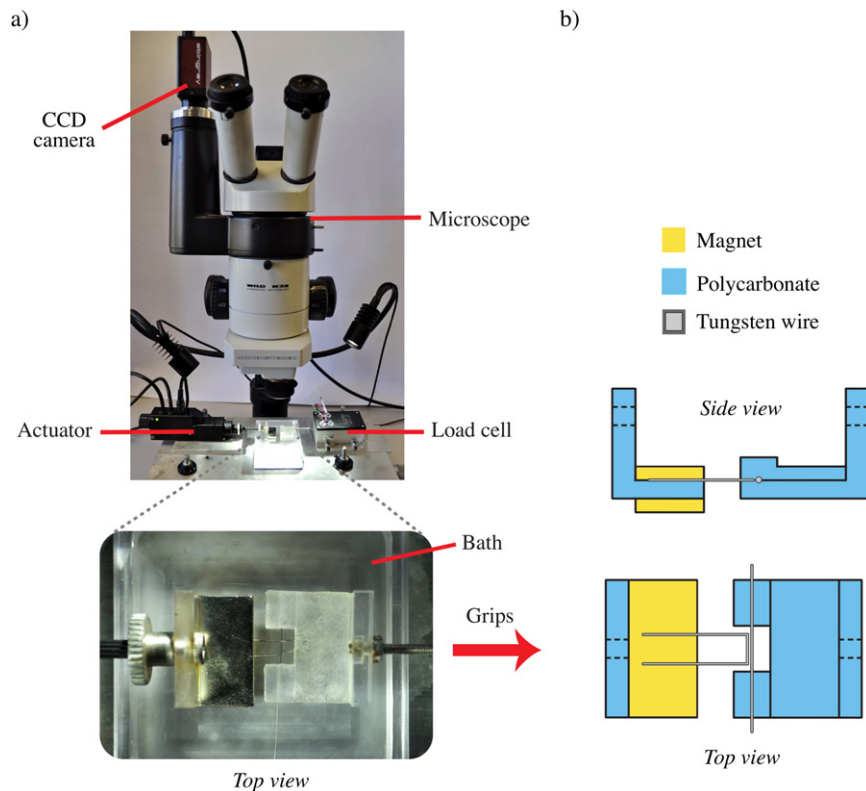


Figure 5. (a) Picture of the testing apparatus including bath and grips. (b) Schematic of the grips.

direction. The load was measured using a low input/high output load cell (Omega 200 g) having a maximum capacity of 200 g, accuracy of ± 0.2 g. The data acquisition rate for the load cell was set to 25 Hz. The specimens were displaced until failure using a microscale linear actuator (Zaber T-NA), which was capable of a minimum step size of $0.0238 \mu\text{m}$, a minimum speed of $0.22 \mu\text{m s}^{-1}$ and a maximum speed of $8000 \mu\text{m s}^{-1}$. Specifically, during testing the displacement rate was $0.5 \mu\text{m s}^{-1}$.

Custom grips were built to hold the ring specimens during testing. The grips were made primarily of polycarbonate with $150 \mu\text{m}$ diameter tungsten wire used to hold the specimens. The grip connected to the actuator was an L-shaped piece of polycarbonate with two magnets that secured the tungsten wire, which was bent to form two right angles as depicted in figure 5(b). The grip connected to the load cell was made of two sandwiched pieces of polycarbonate, one of which was L-shaped. Between the two sandwiched components, a groove was machined in which a straight tungsten wire was threaded and a portion of polycarbonate was removed, as shown in figure 5(b).

The specimens were submerged in a custom built bath containing Ringer's solution to maintain hydration during testing. The bath was placed under a microscope (Heerbrugg Wild M3Z) with $40\times$ magnification and illuminated via two LED lamps (Schott Fibre Optics Ltd). The deformation of the specimen surface was recorded using a CCD camera (Allied Vision Technologies Stingray) at a rate of 25 fps and image size of 1032×776 px, with a field of view of roughly 1.2×1.4 mm. Video, force and displacement data

were recorded synchronously to a desktop computer via a data acquisition module (National Instruments NI cDAQ-9172) using LabVIEW software (National Instruments LabVIEW).

2.3. Strain and stress analyses

A preload (avg = 0.002 N) was applied to flatten the surface of each ring specimen, which was initially cylindrical, in the radial direction (figure 4(b)) and to minimize out of plane motion during tensile testing. Stress and strain were calculated referenced from the preloaded configuration. Engineering strain of the ring sections throughout a trial was calculated using the Digital Image Correlation (DIC) method implemented in Matlab [5]. This non-contact strain measurement method has been successfully used for gathering full two-dimensional strain fields in complex biological materials [24]. For our samples, we chose strain values in a line grid consisting of 30 points in the central portion of the specimens along the radial direction. This central portion was chosen to avoid stress concentration effects induced by the grips. The engineering strain of the specimen was then found by taking the average of the engineering strains computed between pairs of adjacent points along this line grid.

The nominal stress, S , was calculated using the following relationship:

$$S = \frac{L}{tw} \quad (1)$$

where L is the load (measured from a preloaded state) and t and w are the specimen thickness and width, respectively, as indicated in figure 4(a).

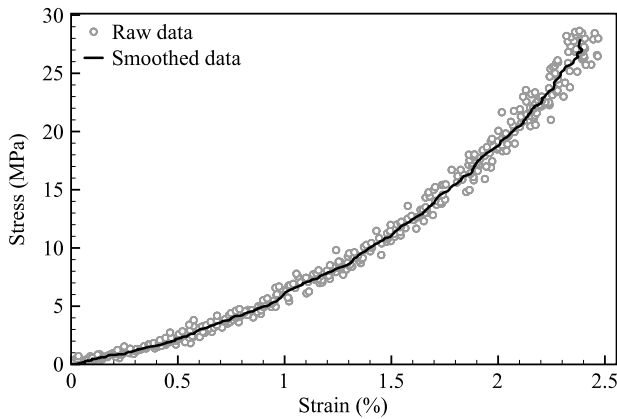


Figure 6. Typical stress–strain curve of one ring specimen of tracheal tube.

Table 1. Mechanical properties determined by testing 30 sections of tracheal tubes.

Parameter	Mean	Standard deviation
Elastic modulus (MPa)	1660	512
Ultimate tensile strength (MPa)	23.7	7.33
Ultimate strain (%)	2.0	0.7
Toughness (MJ m^{-3})	0.207	0.153

The calculated stress and strain values were used to determine the elastic modulus, ultimate tensile strength, ultimate strain and toughness of each specimen. The elastic modulus was calculated as the slope of the linear region of the stress–strain curve. The ultimate tensile strength and ultimate strain were calculated as the magnitude of stress and strain, respectively, before the load was observed to decrease, indicating the occurrence of damage in the specimens. Toughness was measured by calculating the area under the stress–strain curve using a midpoint numerical integration scheme implemented in Matlab. Prior to all analyses, the raw stress and strain data were smoothed using 3- and 19-point running averages, respectively.

Shear stress and out of plane motion of the ring specimens were often observed during tensile testing. Shear occurred mainly in sections of tracheal tubes whose taenidia were imperfectly aligned with the direction of loading. Out of plane motion was due to changing cross-sectional shape of the specimen as it was loaded in tension. Indeed, although we applied an initial preload to flatten the sample (figure 4(b)), in some cases there was additional deflection in the vertical axis orthogonal to the loading direction. In such trials, the speckled points on the specimen surface moved in and out of the focal plane, substantially increasing the error in the DIC analysis. Therefore, data collected from tensile tests in which either shear or bending deformation was detected were discarded. A total of 114 ring tests were conducted, and 30 tests (from $n = 11$ roaches) were deemed sufficient for analysis.

3. Results

The typical stress–strain data obtained by performing ring tests of sections of tracheal tubes are shown in figure 6. One

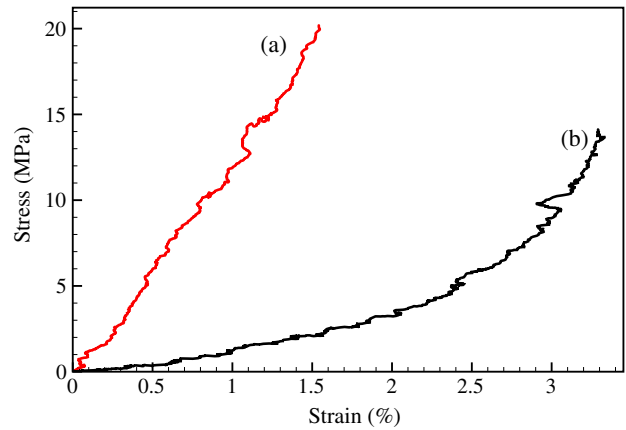


Figure 7. Examples of linear (a) and nonlinear (b) stress–strain curves of two ring specimens.

could clearly observe that the mechanical response of tracheal tubes in the radial direction exhibited some nonlinearities. In particular, there was evidence of strain stiffening, in which a region of low elastic modulus at low strains was followed by a region of increasing elastic modulus at high strains. Moreover, the stress–strain curve appeared to become linear as the strain increased. However, it must be noted that, for some specimens, the stress–strain curves were almost linear with a near-constant elastic modulus (figure 7).

The mode of failure of the specimens during mechanical testing appeared to be determined by slight difference in the geometry of the tracheal tubes. In particular, variance in the diameter of the ring sections of tracheal tubes across their width often caused stress concentration, which produced tears in the region of least diameter. These tears would then propagate, resulting in a gradual failure. Specimens that had an almost uniform diameter along their width failed nearly instantaneously and abruptly. In most of the tests, the mode of failure was a combination of these two modes of failure with an initial gradual tear followed by an abrupt failure of the specimen. The specific mode of failure affected the values of the elastic modulus, ultimate tensile strength, ultimate strain and toughness (table 1).

For specimens that exhibited abrupt failure, the elastic modulus and ultimate tensile strength were higher, but the ultimate strain was lower. In contrast, specimens that failed in a gradual manner exhibited lower ultimate tensile strengths and ultimate tensile strengths, but with higher elastic modulus. The variability in the overall mechanical response across all specimens is shown in figure 8. The variability in the stress value increased as the strain increased due to the different mechanisms of failure previously described. The decrease in the average stress at strains approximately higher than 1.3% is a consequence of the early failure of some specimens during testing.

4. Discussion

This study examines the material properties of tracheal tubes of the American cockroach. Using a new experimental testing

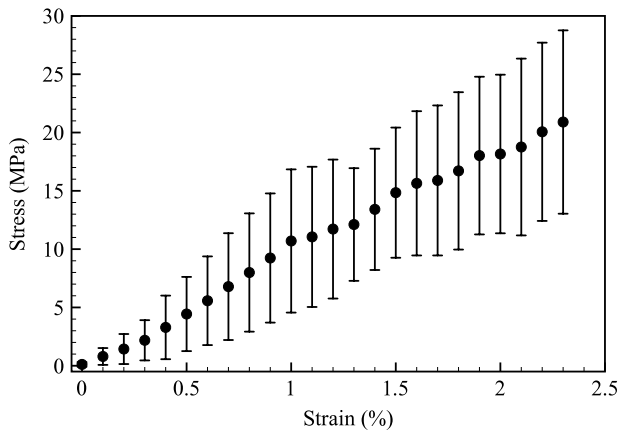


Figure 8. Average stress–strain curve compiled from the stress–strain curves collected from the thirty specimens tested. In this curve, the average stress at 0.1% intervals of strain is shown, with error bars representing one standard deviation about the mean.

device designed to test ring sections, we determined the stress–strain behavior of the main thoracic tracheae in the radial direction. These data were used to broadly characterize cockroach tracheal tissue in terms of elastic modulus, ultimate tensile strength, ultimate strain, and toughness. To our knowledge, this work represents the first quantification of the mechanical properties of insect tracheal tubes.

The mechanical properties of tracheal tubes can be compared to those of other forms of insect cuticle. Many structural elements in the insect body are composed of cuticle, a biological composite consisting of chitin fibers (a polysaccharide), various proteins, and other elements such as lipids and metals [19]. The different roles that cuticle plays in the insect body are manifest in their mechanical properties, which can vary widely depending on the volume fraction and arrangement of chitin and the components of the supporting matrix material. The water content is especially important in the resulting properties of the cuticle, as a 5% reduction in the water content can result in as large as a 10 fold increase in its elastic modulus [14]. Over the body of the insect, the stiffness varies from 1 kPa in the soft cuticle of a larva, to the order of MPa in untanned cuticle, and up to 20 GPa for tanned, dry cuticle [19]. The cockroach tracheal tubes in our study exhibited a mean elastic modulus of 1.5 GPa, which is within the range of elastic moduli of untanned puparium tissue [19]. Both of these materials are hydrated chitin composites that need to be stiff enough to maintain shape, but compliant enough to allow for the appropriate amount of movement.

The main thoracic tracheal trunks of American cockroaches exhibited nonlinearities in stress and strain when loaded in tension, with a region of low elastic modulus at low strains, followed by a nearly linear region of higher elastic modulus at higher strains. This strain stiffening is a common feature of soft biological materials [7]. The causes of the observed nonlinearity in the response of the tracheal tubes are unknown, but are possibly related to the structural arrangement of their components both at the micro- and macroscales.

Changes in configuration of microscale structural fibers are a known source of nonlinearity in many biological

materials [7]. Thus, although no micro-structural analysis has been performed on tracheal tubes, it is reasonable to think that changes in the arrangement of the supporting chitin fibers under tensile loading contribute to the observed nonlinear behavior. Chitin fibers are oriented tangentially to the tracheal wall and wind circumferentially with the taenidia. This configuration is likely to be altered during tensile loading from an undeformed state in which there are gaps between adjacent fibers to a deformed state where the fibers are closely packed. Future studies should include detailed micro-structural investigations of tracheal tubes to explain the observed nonlinearity during tensile loading.

The surface of ring sections of tracheal tubes was initially almost cylindrical and flattened out under loading in the radial direction (figure 4(b)). To minimize the out of plane motion of the specimens in the direction perpendicular to the lens of the camera used in the experimental setup, a preload was applied. It must be noted that the results of the trials, in which the out of plane motion was detected even after preload, were removed from the data reported in this study. In addition, small out of plane motion, due to the non-planar configuration of the specimens, may have occurred even after pre-loading the specimens. Such motion may have influenced the strain measurements and contributed to the reported nonlinearity in the data.

There was considerable variation in the mechanical properties reported here, likely rooted in the complex geometry and composition of the tracheal tubes. Although we attempted to standardize the shape and size of ring specimens, some tubes showed non-uniform diameters, which would unevenly distribute the load during the tensile test. Furthermore, tube thickness may have varied along the length, resulting in stress concentrations in the thinnest portions of the tube wall. The taenidial patterns were also variable, and taenidial angle and density were not quantified. In particular, specimens with slightly misaligned taenidia exhibited out of plane motion and shear during a test. Lastly, the per cent composition of components such as chitin fibers likely have a strong effect on tube material properties. The influence of such tracheal tube morphological characteristics will be examined in future studies.

The ring tests conducted in this study represent the first step toward a complete mechanical characterization of insect tracheal tubes. Indeed, although the tests provided important information on the mechanical properties of the tubes, they lack the ability to describe the three-dimensional mechanical response of these tubes during respiration. In particular, the collapse of tracheal tubes in real insects involves loading regimes as shown in figure 1 that are different from the tensile loading reported here. We are currently designing a new mechanical testing device and conducting new experiments on the tracheal tubes to better emulate the three-dimensional physiological loading conditions. The inhomogeneity of the tracheal tubes determined by their constituents and mutual arrangement poses a challenge in the evaluation of their mechanical properties. However, it is speculated that this inhomogeneity is responsible for the rhythmic and selective collapse behavior of tracheal tubes in RTC. For this reason,

three-dimensional stress and strain analyses of the tubes coupled with micro-structural studies will ultimately offer the knowledge needed to mimic the respiratory system in bio-inspired devices.

Acknowledgments

This research was supported by NSF grant #0938047 and the Virginia Tech Institute for Critical Technology and Applied Science (ICTAS). The authors thank Dr Donald E Mullins of the Department of Entomology at Virginia Tech for donating the cockroaches used in this study, Laura Clatterbuck, an undergraduate student of the Department of Biology at Virginia Tech, who helped with the dissection of the tracheal tubes, and Sean Smith, an undergraduate student of the Department of Mechanical Engineering at Harding University, who helped with the validation of the testing apparatus using rubber o-rings.

References

- [1] Arena P, Fortuna L, Frasca M, Patane L and Pavone M 2005 Climbing obstacles via bio-inspired CNN-CPG and adaptive attitude control *ISCAS 2005: IEEE Int. Symp. on Circuits and Systems 2005* pp 5214–7
- [2] Cham J G, Karpick J K and Cutkosky M R 2004 Stride period adaptation of a biomimetic running hexapod *Int. J. Robot. Res.* **23** 141
- [3] Chapman R F 1998 *The Insects: Structure and Function* (Cambridge: Cambridge University Press)
- [4] Cox A, Monopoli D, Cveticanin D, Goldfarb M and Garcia E 2002 The development of elastodynamic components for piezoelectrically actuated flapping micro-air vehicles *J. Intell. Mater. Syst. Struct.* **13** 611
- [5] Eberl C, Thompson R and Gianola D 2006 Digital image correlation and tracking with Matlab *Matlab File Exchange* <http://www.mathworks.com/matlabcentral/fileexchange/12413>
- [6] Evans D L and Schmidt J O 1990 *Insect Defenses: Adaptive Mechanisms and Strategies of Prey and Predators* (New York: State University of New York Press)
- [7] Fung Y 1993 *Biomechanics: Mechanical Properties of Living Tissues* (Berlin: Springer)
- [8] Klowden M J 2002 *Physiological Systems in Insects* (San Diego, CA: Academic)
- [9] Krogh A 1920 Studien Über Tracheenrespiration. II. Über Gasdiffusion in den Tracheen *Pflügers Arch.* **179** 95–112
- [10] Lehman R M, Lundgren J G and Petzke L M 2009 Bacterial communities associated with the digestive tract of the predatory ground beetle, poecilus chalcites, and their modification by laboratory rearing and antibiotic treatment *Microbial. Ecol.* **57** 349–58
- [11] Locke M 1957 The structure of insect tracheae *Q. J. Microsc. Sci.* **98** 487–92
- [12] McIntosh A and Beheshti N 2008 Insect inspiration *Phys. World* (April) 29–31
- [13] Pickard W 1974 Transition regime diffusion and the structure of the insect tracheolar system *J. Insect Physiol.* **20** 947–56
- [14] Reynolds S E 1975 The mechanical properties of the abdominal cuticle of *Rhodnius* larvae. *J. Exp. Biol.* **62** 69
- [15] Socha J J, Förster T D and Greenlee K J 2010 Issues of convection in insect respiration: insights from synchrotron x-ray imaging and beyond *Respir. Physiol. Neurobiol.* **173** S65–73
- [16] Socha J J, Lee W K, Harrison J F, Waters J S, Fezzaa K and Westneat M W 2008 Correlated patterns of tracheal compression and convective gas exchange in a carabid beetle *J. Exp. Biol.* **211** 3409
- [17] Socha J J, Westneat M W, Harrison J F, Waters J S and Lee W K 2007 Real-time phase-contrast x-ray imaging: a new technique for the study of animal form and function *BMC Biol.* **5** 6
- [18] Vincent J F V 2002 Arthropod cuticle: a natural composite shell system *Composites A* **33** 1311–5
- [19] Vincent J F V and Wegst U G K 2004 Design and mechanical properties of insect cuticle *Arthropod Structure Development* **33** 187–99
- [20] Waldbauer G 2006 *A Walk Around the Pond: Insects in and Over the Water* (Cambridge, MA: Harvard University Press)
- [21] Weis-Fogh T 1964 Diffusion in insect wing muscle, the most active tissue known *J. Exp. Biol.* **41** 229
- [22] Westneat M W, Betz O, Blob R W, Fezzaa K, Cooper W J and Lee W K 2003 Tracheal respiration in insects visualized with synchrotron x-ray imaging *Science* **299** 558
- [23] Wood R J 2008 The first takeoff of a biologically inspired at-scale robotic insect *IEEE Trans. Robot.* **24** 341–7
- [24] Zhang D and Arola D D 2004 Applications of digital image correlation to biological tissues *J. Biomed. Opt.* **9** 691